A magnetic graphitic carbon nitride as a new adsorbent for simple separation of Ni (II) ion from foodstuff by ultrasound-assisted magnetic dispersive-micro solid phase extraction method

Bahareh Fahimirad[a] and Alireza Asghari[a]*

[a] *Department of Chemistry, Semnan University, Semnan, Iran*

ABSTRACT

In this research, a magnetic graphitic carbon nitride (g-C_3N_4-$SnFe_2O_4$) was successfully synthesized and utilized as an efficient adsorbent for nickel (Ni^{2+}) separation/extraction from vegetable samples by ultrasound-assisted magnetic dispersive micro solid-phase extraction (UA-M-D-μSPE). After separation and preconcentration step, Ni ions were determined via micro-sampling flame atomic absorption spectrometry (MS-FAAS). A successful synthesis of g-C_3N_4-$SnFe_2O_4$ was investigated by Fourier transform infrared spectroscopy (FT-IR), X-ray diffraction (XRD), field emission scanning electron microscopy (FE-SEM), and vibrating sample magnetometer (VSM). The optimization of adsorption and desorption steps was effectively studied by the on-at-a time method. In addition, under the optimum experimental conditions, the limits of detection (LODs), the linear ranges (LR) and relative standard deviations (RSDs%, for n = 5) were obtained 1.0 μgL^{-1}, 4.0 ─ 500.0 μgL^{-1}, and 1.4 respectively.

1. Introduction

One of the important category of foodstuff is Vegetables. This category of foodstuff contain vitamins, anti-oxidants, minerals, and diverse beneficial phytochemicals[1, 2]. In presence of heavy metals in vegetables, even at trace levels, is one of health concern from industrial wastewater [3]. Among a variety of metal ions, nickel is toxic, even at trace levels [4-6]. Different methods use for determination of this metal ion such as flame atomic adsorption spectrometry (FAAS),

electrothermal atomic adsorption spectrometry (ETAAS), inductively coupled plasma-optical emission spectrometry (ICP-OES), and inductively coupled plasma-mass spectrometry (ICP-MS)[7]. But micro-sampling-FAAs (μ-FAAs) due to low cost which requires a low operational facility, and uses a small volume of the eluent, has recently been very much considered [7].

In any case, the use of these methods to measure low-nickel amounts is not suitable because of their low sensitivity. Therefore, the sample preparation step is required before the measurement by the μ-FAAs [8]. Among the various types of sample preparation

methods, solid phase extraction (SPE) is very much appreciated due to its simplicity, low cost, high speed; moreover, the solid phase extraction requires low amounts of reagents, a high recovery, environmentally friendly, and a low organic solvent consumption [9, 10]. The ultrasound-assisted dispersive magnetic solid-phase extraction (UA-DM-SPE) is a new form of SPE which leads to more rapidity and ease of operation compared with the conventional SPE. In this method, using ultrasonic waves, the contact surface of the adsorbent with the analyte is increased in a very short time, as well as due to the adsorbent magnetic property, the centrifuge step is removed and the process of separation and preconcentration is performed in short time [8]. As a result, in this method use a novel nanoadsorbents with a high adsorption efficiency and the easy separation is an important step. A graphitic carbon nitride (g-C_3N_4) is a new form of organic polymer-like material, and due to its quick and facile synthesis, special structure, and low cost has been a lot touched recently [11]. The g-C_3N_4 sheets can be used as SPE sorbents, but they have several problems, such as Re-aggregation of the nanosheets, and also their low surface area [12]. Therefore, to raise any of the characteristics of this compound and rapid separation of it from sample solution, nanomagnetic of $SnFe_2O_4$ was used for increasing of surface area and separation of g-C_3N_4 of the solution.

Therefore, in this work, the nanoadsorbent g-C_3N_4-$SnFe_2O_4$ with a very high absorption power as an efficient nanoadsorbent for ultrasound-assisted magnetic dispersive micro solid-phase extraction (UA-M-D-μSPE) was synthesized and applied for the separation and preconcentration of the Ni (II) ion and toxic metal ion was measured using the micro-sampling flame atomic adsorption spectrometry (μS-FAAS) technique.

2. Experimental Procedure

2.1. Materials

All the reagents used in this work including melamine, Ni $(NO_3)_2 \cdot 3H_2O$, $SnCl_2 \cdot 2H_2O$,

$FeCl_3 \cdot 6H_2O$, HCl (37%), HNO_3, NaOH, H_2SO_4, and ethanol were of the highest available purity, supplied from Merck Company. Standard solution was prepared by dissolving appropriate amounts of Ni $(NO_3)_2$. In addition, $3H_2O$ in doubly distilled water at a concentration of 1000 mg L^{-1}. Working standard solutions with intermediate concentrations were prepared daily by dilution of the stock solutions.

2.2. Instrumentation

For determination of Ni(II) in the samples, an Agilent model 240 AA Shimadzu (USA) flame atomic adsorption spectrometer was used with the Ni hollow cathode lamps as the radiation sources. The pH values of the solutions were adjusted by a pH meter, PHS-3BWModel (Bell, Italy) with a glass combination electrode. An ultrasonic bath (SW3, Switzerland) was used at a frequency of 50/60 kHz to dissipate adsorbent in a sample solution.

Fourier transform-infrared (FT-IR) spectra using a Shimadzu 8400s spectrometer were determined in the range of 400-4000 cm^{-1}. Scanning electronmicroscopy (FE-SEM) analysis was carried out using a Tescanvega II XMU Digital Scanning Microscope. Energy-dispersive X-ray spectroscopy elemental analysis (EDX) of the samples was obtained using a Philips XL-30 energy-dispersiveX-ray spectroscope. X-ray diffraction (XRD) patterns were obtained on a Burker AXS (Model B8-Advance). The magnetic properties were analyzed using a vibrating sample magnetometer (VSM, Lakeshore7407) at room temperature.

2.3. Synthesis of g-C_3N_4-$SnFe_2O_4$

3 g of melamine was placed in a crucible and hated in 520 ^{0}C with a rate of 10 ^{0}C/min for 4 hours. Finally, yellow g-C_3N_4 precipitate was formed. In the next step, to synthesis of $SnFe_2O_4$ nanostructure, $SnCl_2 \cdot 2H_2O$ and $FeCl_3 \cdot 6H_2O$ with a stoichiometric ratio of 1:2 were mixed in 100 mL of distilled water

and was heated at 80 ^{0}C. Then pH of the solution was adjusted using NaOH solution in 10. After 3hours, a black precipitate of $SnFe_2O_4$ was formed. A black precipitate was collected by an external magnetic field, and repeatedly washed with ethanol and distilled water. Finally, the black precipitate was dried at 120 ° C for 24 h. To synthesis of the g-C_3N_4-$SnFe_2O_4$ nanoadsorbent, 0.13 g of g-C_3N_4 whit 0.2 g of the $SnFe_2O_4$ nanostructure was homogeneously mixed by grinding in an agate mortar for 30 min and then the powder was calcined in a furnace at 400 ^{0}C for 4 hours [13].

2.4. Preparation of real samples

The vegetable were provided from Tehran markets in Iran. The vegetables were cut into small pieces, washed with deionized water. Then, the samples were dried in an oven for 24 hours. 25 mL of HNO_3 (65%) was added to 1.2 gr of each sample and placed in acid overnight. Then the samples were heated at 250 ^{o}C, until their liquid contents were evaporated, and they became almost dried. In order to complete the digestive process, 5 mL of H_2O_2 (30%) was added to the samples and then heated to vaporize their liquid contents. Afterwards, the samples were washed with deionized water and heated to boil the solutions. Then the contents were cooled and transferred to sample flask of 25 mL, and diluted with deionized water to 25 mL. Finally, the pH values for the solutions were adjusted, and certain amounts of the metal ions were spiked.

2.5. Procedure for magnetic dispersive micro solid-phase extraction

10.0 mg nanoadsorbent was added to 10.0 mL of sample solution in a glass vial containing containing 50.0 μgL^{-1} of Ni (II) at a pH value of 6.0. The solution was sonicated for 5 min at 25±3 ^{o}C, and then the nanoadsorbent was separated from the solution by a magnetic field within 2 min. In the desorption step, 250 μL of HNO_3 (3 $molL^{-1}$) was added to the sample solution, and sonicated

for 4 min. Then, HNO_3 solution as the eluent was collected and then injected into FFAS by means of a micro-sampler for determining the metal ions. The extraction recovery (ER), and relative recovery (RR) for each metal ion were calculated as:

$$ER = \frac{n_{inj}}{n_0} \qquad (1)$$

where C_{inj} is the concentration of the metal ions in 200 μl eluent (in the desorption step), and c_0 is the initial concentration of the metal ions.

$$RR = \frac{C_{found} - C_{real}}{C_{added}} \times 100 \qquad (2)$$

where c_{found}, c_{real}, and c_{added} are the concentration of the analyte after adding the standard to the real sample, concentration of the real sample, and concentration of the standard solution which was injected to the real sample, respectively[14].

3. Results and discussions

3.1. Characterization of synthesized nanoadsorbent

The crystalline structures of g-C_3N_4, $SnFe_2O_4$, and g-C_3N_4-$SnFe_2O_4$ were determined by XRD. In Fig.1a, two typical diffraction peaks can be observed at 2Θ= 27.47 and 13.51^0 for pure g-C_3N_4, which represent the inter-planar graphitic stacking; these peaks well-agreed with the values in the standard card (JCPDF 87-1526). Also, in Fig 1b, the peaks at 2Θ=20.18, 23.31, 33.23, 37.26, 39.2, 40.98, 47.71, 53.75, and 59.38 confirm $SnFe_2O_4$. Also Fig. 1c confirms the formation of the g-C_3N_4-$SnFe_2O_4$ composite according to reference[8]. The FT-IR spectra in Fig 2a shows the peaks for pure g-C_3N_4 at 1241,1319, and 1409 cm^{-1} can be attributed to aromatic C-N stretching and the peak at 810 cm^{-1} can be attributed to triazine units and also, the peaks at 1568 and 1650 cm^{-1} can be related to C=N stretching [15, 16]. The adsorption peak in Fig. 2 b at 570 cm^{-1} can be attributed to the stretching vibrations of the Sn–O and Fe–O bonds [17]. Finally, the index peaks in Fig. 2c confirm
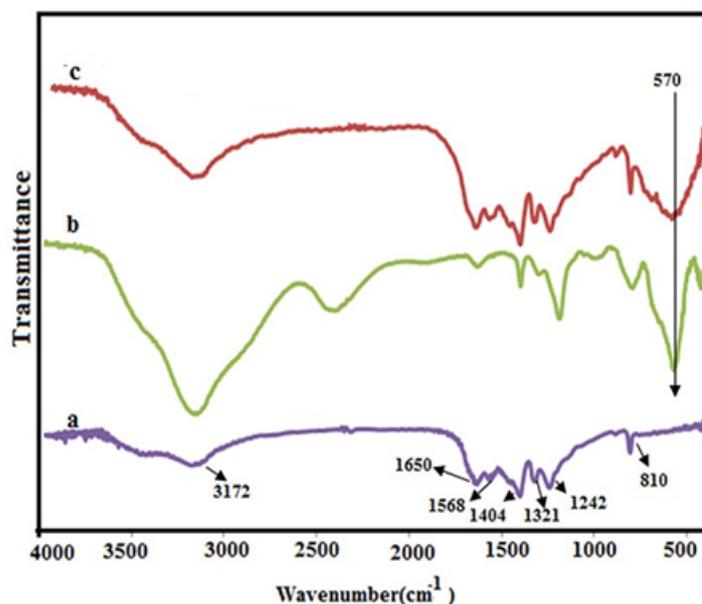
Fig. 1. FT-IR spectra of (a) g-C_3N_4 , (b) $SnFe_2O_4$, and (c) g-C_3N_4- $SnFe_2O_4$.

the formation of the g-C_3N_4-$SnFe_2O_4$ compound. The FE-SEM micrographs for the nanostructures g-C_3N_4 and g-C_3N_4-$SnFe_2O_4$ are shown in Figs. 3a and b. According to these figures, the $SnFe_2O_4$ nanostructure is cubic with a quite uniform size of about 60-120 nm. The Fig 3b shows that the cubic particles of $SnFe_2O_4$ are uniformly distributed on the g-C_3N_4 surface. The magnetic properties of the synthesized nanoadsorbent was investigated through a vibrating sample magnetometer (VSM) at room temperature. Fig. 4 show the magnetic hysteresis curve for $SnFe_2O_4$ and g-C_3N_4-$SnFe_2O_4$ in an applied magnetic field. The maximum saturation magnetization (Ms) values of $SnFe_2O_4$ and g-C_3N_4-$SnFe_2O_4$ were found to be 4.87 and 3.14 emu g^{-1} respectively. The results of this analysis show that synthesized nanoadsorbent has a good magnetic strength, and that it can be separated easily from the aqueous solution with the help of an applied magnetic field.
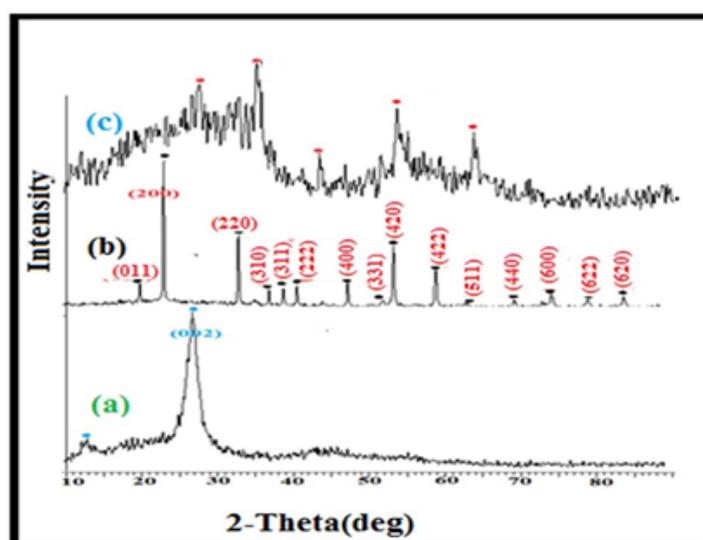
Fig. 2. XRD pattern of (a) g-C_3N_4 (b) $SnFe_2O_4$ and (c) g-C_3N_4- $SnFe_2O_4$.
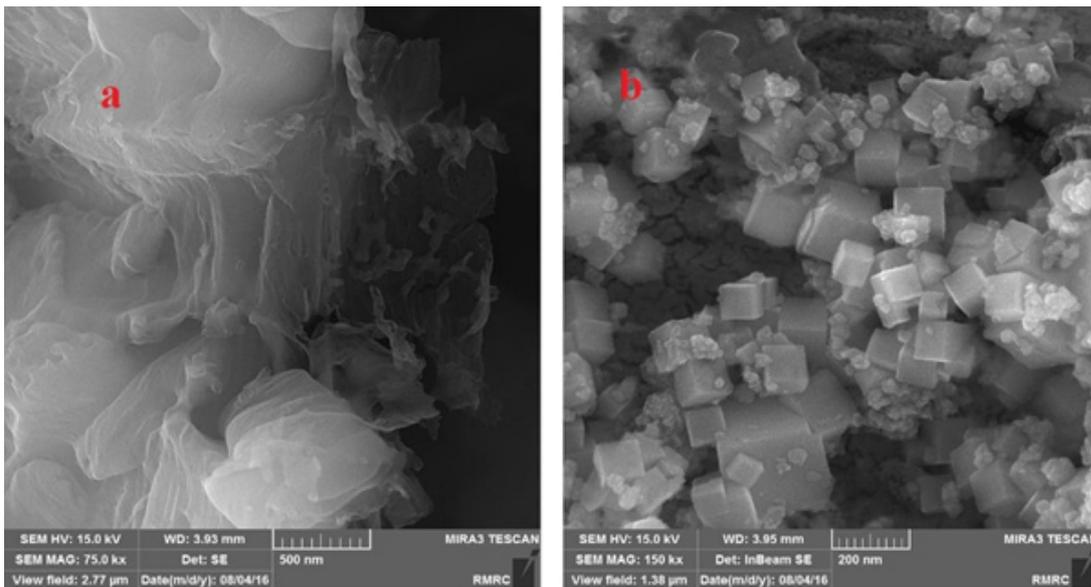
Fig. 3. SEM image of (a), g-C$_3$N$_4$ and (b) g-C$_3$N$_4$- SnFe$_2$O$_4$.

3.2 Optimization of experimental conditions

To investigation of effective parameters, in adsorption step, first 10 mL of solutions containing metal ions with concentration of 10 µgL^{-1} were prepared and a certain amount of adsorbent was added to it. Then, pH of solutions was set using HCl or NaOH solutions (0.1 molL^{-1}) and the solution was ultrasound for a specific time. Then adsorbent was separated by using magnetic field. In desorption step, the certain volume of eluent was added to

adsorbent, and the solution was ultrasound for a specific time. In this step, Ni (II) was desorb in to eluent, and finally was injected to FAAs by using micro-sampling device.

3.2.1 Effect of solution pH, adsorbent amounts, and ultrasonic time in adsorption step

The solution pH was investigated in the range of 3 to 8. The results in Fig. 5a show that in pH 6, the most recovery is achieved. In acidic pH values, there is a strong competition
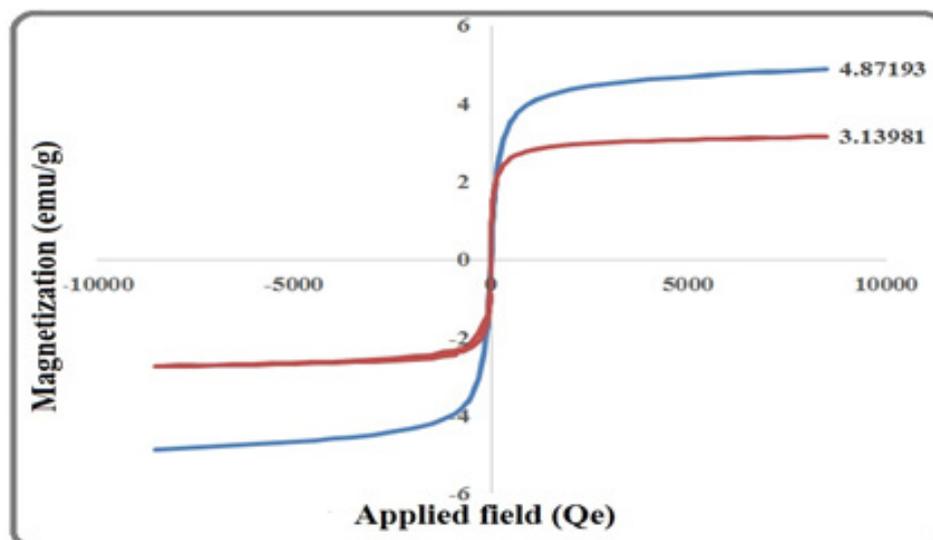
Fig. 4. Magnetization curves of (a), SnFe$_2$O$_4$ and (b) g-C$_3$N$_4$- SnFe$_2$O$_4$.
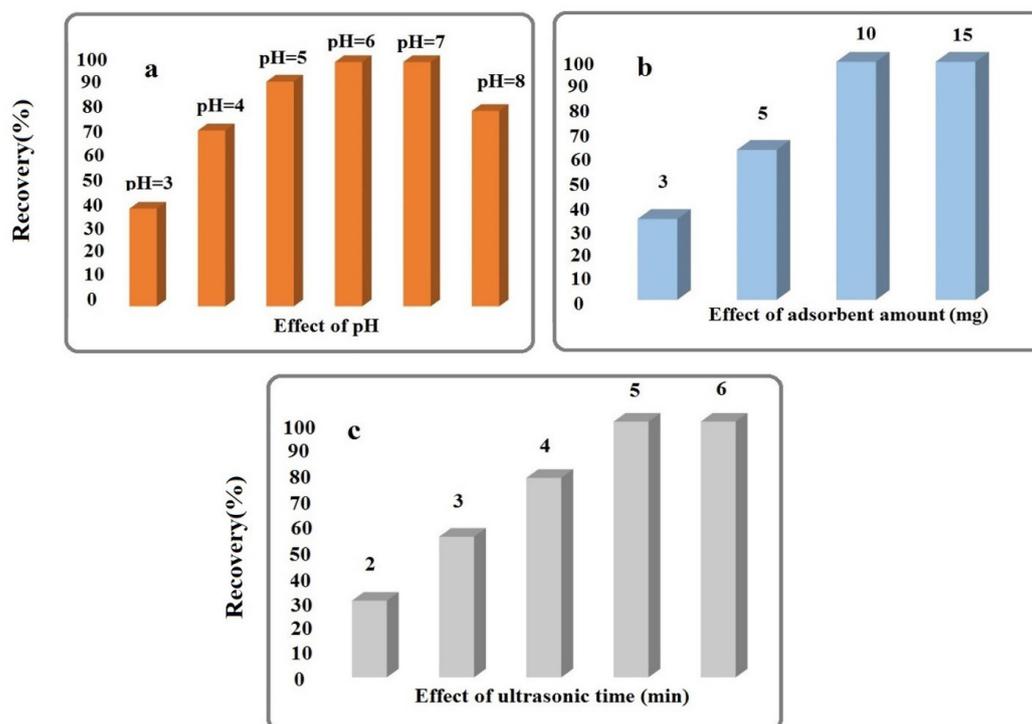
Fig. 5. The effect of effective parameters on the recovery percentage of Ni(II) ion in adsorption step.

between H^+ ions and metal ion, as the result in pH less than pH of 6, the recovery of metal ion adsorption decrease. On the other hand, in basic pH values, by increasing of OH concentration in sample solution, 1) the active sits on the adsorbent surface (OH and NH groups), due to the formation of the hydrogen bond, deactivated and as a result the recovery reduce; 2) the reduction in recovery can be attributed to the formation of the precipitation of some ion in the form of hydroxides [8]. The adsorbent amounts was investigated in range of 3 to 15 mg. The results in Fig 5b shows that an absorbent amount of 10 mg of nano adsorbent for the metal ion lead to most recovery. The effect of ultrasonic time was investigated on the recovery of metal ions in rang 2 to 6 min. According to the results shown in figure 5c, the time of 5 min was selected as optimum time.

3.2.2 Effects of type, concentration, and volume of eluent, and ultrasonic time at the desorption step
The eluents including HCl, HNO_3 and H_2SO_4 were investigated on the recovery. The results in Fig 6a show that HNO_3 for metal ion has as better eluent. The concentration of eluent and the volume of eluent were investigated in rang 1 to 4 $mol.L^{-1}$ and in rang of 100 to 300 µL, respectively. According to figure 6b and 6c the optimum concentration and volume of eluent were obtained 3 $mol.L^{-1}$ and 250 µL of the eluent. The effect of ultrasonic time was investigated in rang 2 to 5 min. The results in Fig 6d show that by increasing of ultrasonic time to 4 min the recovery of metal ion increase and then the recovery is stationary. The result indicates that the best time for this step was 4 minutes.

3.3. Analytical validation
Under the optimized experimental conditions, the linear ranges with determination coefficient (r^2) of
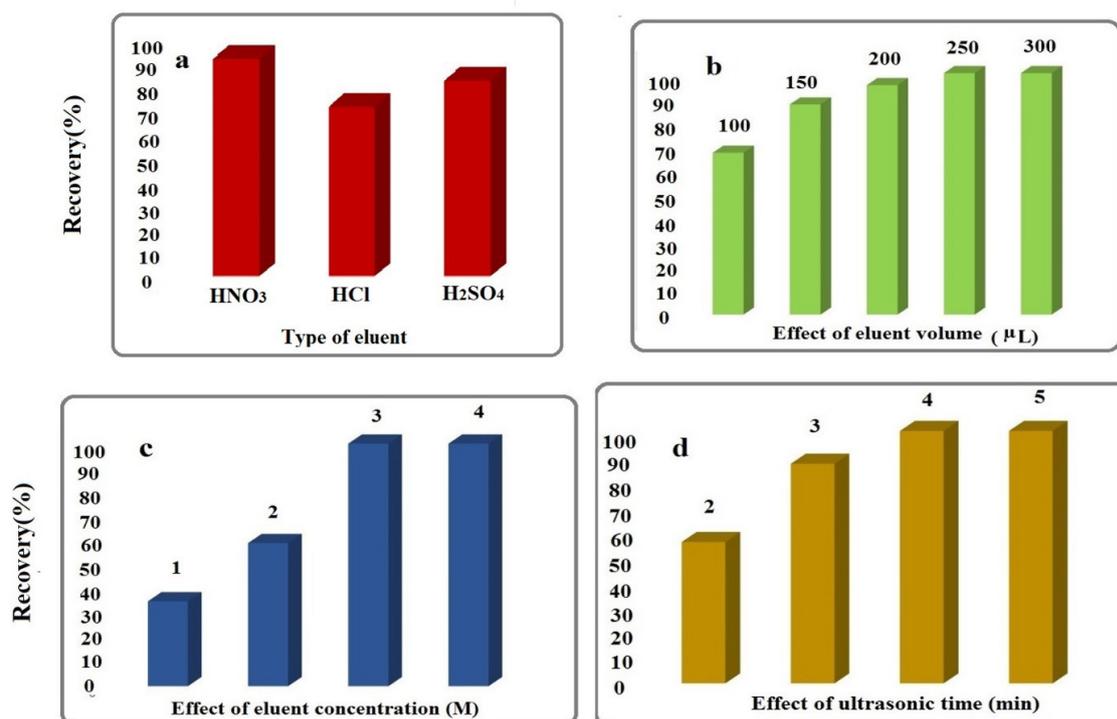
Fig. 6. The effect of effective parameters on the recovery percentage of Ni(II) ion in desorption step.

calibration 0.996 were obtained between 4.0-500.0 μg L^{-1}. Limit of detection (LOD) for five replicates were calculated 1.0 μg L^{-1}.

Also, the relative standard deviations (RSDs) were obtained for 5 repetitions, and were 1.4%. Finally, the results indicate that the proposed method has a good precision for the separation and preconcentration of trace amounts of Ni (II) ions.

3.4. Application of method in real samples

Considering the importance of measuring of heavy metals such as Ni(II) ion in vegetables, hence in the present work, the proposed method was used to determination and extraction of Ni ion in the samples of Leek, Lettuce, Parsley, and Radish. For this purpose, in the obtained optimum condition, the method was done in real samples, and relative recovery (RR) was calculated for Ni (II) ions according to the equation (2). The results in Table 1 show that measured amounts are in good agreement with added amounts of Ni (II) ions. Finally, the obtained results confirm the good high ability of

Table 1. Levels of metal ions in real samples.

Sample	[a]Ni (II)		
	Added (μg L^{-1})	(found-real) (μg L^{-1})	[b]RR (%)
Leek		BDL	
	50	49.0±1.5	98.0
Parsley		BDL	
	50	49.5±1.3	99.0
Radish		BDL	
	50	50.0±1.5	100.0
Lettuce		BDL	
	50	48.8±4.0	97.6

[a] Mean of three determinations ± confidence interval (P = 0.95, n =5)
[b] Relative Recovery

Table 2. Effect of potentially interfering ions on recovery of metal ions.

Potentially interfering ions	Tolerance limit[a] (C_i/C_a)	Recovery%
		Ni(II)
Na^+	1000	99.00
Mg^{2+}	1000	100.00
NO^{3-}	1000	99.00
Cl^-	1000	99.40
Zn^{2+}	600	98.83
Al^{3+}	500	98.50

[a] Concentration ratio of potentially interfering and analyte ions. Adsorption conditions: 10 mg of adsorbent, pH=6. Desorption conditions: 250 μL of HNO_3 with concentration of 3 mol L^{-1}.

the method for determination trace concentration of Ni ion in real samples.

3.5. Effect of foreign species on the recovery

In the optimum condition, the effects of the foreign ions was investigated on the UA-M-D-μSPE method. The tolerance limit is defined as the concentration that results in a change of ±5% in the recoveries. Accordingly, the results in Table 2 indicate that the common ions with high concentrations in real samples do not have a considerable interference effect on the recovery, and the adsorbent can be used for this method without significant matrix effects.

3.6. Comparison methods with other methods of SPE for separation Ni(II).

In order to demonstrate the efficiency of the method, a comparison was done between the proposed method and the other methods. Table 3 shows the type of nanoadsorbent, method, amount of nanoadsorbent, LOD, RSD, and volume of eluent for the extraction and preconcentration of the Ni (II) ions. The results in Table 3 show that maximum recovery in proposed method in compared with the other method was obtained with the least amount of nanoadsorbent. Also, this method is environmentally friendly due to the low use of an elution solvent. This method is also simple and fast. In addition to, compared with the same methods, our method has a low RSD and also the limit of detection this method is comparable to the other methods presented in Table3 .

4. Conclusions

In this work, g-C_3N_4-$SnFe_2O_4$ adsorbent with a

Table 3. Comparison between EA-DM-μSPE and other published methods.

Adsorbent	Metal	Method	Amount of adsorbent (mg)	LOD (ng.mL^{-1})	RSD (ng.mL^{-1})	Final volume of eluent	Ref.
GO–H_2NP^1	Ni(II))	SPE column /FAAS	40	5.4×10^{-3}	-	5.0 mL	[18]
Ion-imprinted polymers	Ni(II)	SPE column /FAAS	200	0.2	2.5	5.0 mL	[19]
DMG/SDS-ACMNPs^2	Ni(II)	SPE /FAAS	200	4.6	1.9	2.0 mL	[20]
Molecularly imprinted polymers	Ni(II)	SPE column /FAAS	575	0.3	5.0	5.0 mL	[21]
g-C_3N_4-$SnFe_2O_4$	Ni(II)	UA-M-D-μSPE /MS-FAAS	10	1.0	1.4	250 μL	This work

[1] Graphene oxide with covalently linked porphyrin
[2] Dimethylglyoxim/sodium dodecyl sulfate-immobilized on alumina-coated magnetite nanoparticles

good activity was successfully synthesized, and its application was investigated for extraction and preconcentration of the Ni (II) ion using ultrasound-assisted magnetic dispersive micro solid-phase extraction method. Preconcentrated nickel ion was measured with micro sampling flame atomic adsorption spectroscopy.

The most important benefits of this method are: low time (9 min), low volume of eluent (250 μL), and low amount of adsorbent (10 mg). Finally, the results obtained showed that the method had low LODs, a high recovery in a short time, and a good preconcentration factor due to the use of a low amount of eluent for trace amounts of the understudied ions.

5. Acknowledgment

6. Nomenclature

FAAS: flame atomic adsorption spectrometry

ETAAS: electro-thermal atomic adsorption spectrometry

ICP-OES: inductively coupled plasma-optical emission spectrometry

7. References

[1] B. Demmig-Adams, W.W. Adams, Antioxidants in photosynthesis and human nutrition, Science, 298 (2002) 2149-2153.

[2] L. Ren, Y. Hemar, C.O. Perera, G. Lewis, G.W. Krissansen, P.K. Buchanan, Antibacterial and antioxidant activities of aqueous extracts of eight edible mushrooms, Bioact. Carbohydr. Dietary Fibre., 3 (2014) 41-51.

[3] A. Wilkowska, M. Biziuk, Determination of pesticide residues in food matrices using the QuEChERS methodology, Food. Chem, 125 (2011) 803-812.

[4] M. Ghazaghi, H.Z. Mousavi, A.M. Rashidi, H. Shirkhanloo, R. Rahighi, Innovative separation and preconcentration technique of coagulating homogenous dispersive micro solid phase

extraction exploiting graphene oxide nanosheets, Anal. chim. acta, 902 (2016) 33-42.

[5] L. Zhang, V. Hessel, J. Peng, Q. Wang, L. Zhang, Co and Ni extraction and separation in segmented micro-flow using a coiled flow inverter, Chem. Eng. J, 307 (2017) 1-8.

[6] A.A. Gouda, S.M. Al Ghannam, Impregnated multiwalled carbon nanotubes as efficient sorbent for the solid phase extraction of trace amounts of heavy metal ions in food and water samples, Food. Chem, 202 (2016) 409-416.

[7] B. Barfi, A. Asghari, M. Rajabi, S. Sabzalian, F. Khanalipoor, M. Behzad, Optimized syringe-assisted dispersive micro solid phase extraction coupled with microsampling flame atomic absorption spectrometry for the simple and fast determination of potentially toxic metals in fruit juice and bio-fluid samples, RSC. Adv, 5 (2015) 31930-31941.

[8] B. Fahimirad, A. Asghari, M. Rajabi, A novel nanoadsorbent consisting of covalently functionalized melamine onto MWCNT/Fe_3O_4 nanoparticles for efficient microextraction of highly adverse metal ions from organic and inorganic vegetables: Optimization by multivariate analysis, J. Mol. Liq, 252 (2018) 383-391.

[9] A. Safavi, N. Iranpoor, N. Saghir, S. Momeni, Glycerol–silica gel: a new solid sorbent for preconcentration and determination of traces of cobalt (II) ion, Anal. Chim. Acta, 569 (2006) 139-144.

[10] M. Tuzen, K.O. Saygi, M. Soylak, Novel solid phase extraction procedure for gold (III) on Dowex M 4195 prior to its flame atomic absorption spectrometric determination, J. Hazard. Mater, 156 (2008) 591-595.

[11] K. Vignesh, M. Kang, Facile synthesis, characterization and recyclable photocatalytic activity of Ag_2WO_4@ g-C_3N_4, Mater. Sci. Eng. B, 199 (2015) 30-36.

[12] H.-J. Li, B.-W. Sun, L. Sui, D.-J. Qian, M. Chen, Preparation of water-dispersible porous gC 3 N 4 with improved photocatalytic activity by chemical oxidation, Phys. Chem. Chem. Phys, 17 (2015) 3309-3315.

[13] B. Fahimirad, A. Asghari, M. Rajabi, Magnetic graphitic carbon nitride nanoparticles covalently modified with an ethylenediamine for dispersive

solid-phase extraction of lead (II) and cadmium (II) prior to their quantitation by FAAS, Micro, Chim. Acta, 184 (2017) 3027-3035.

[14] M.R. Sohrabi, Z. Matbouie, A.A. Asgharinezhad, A. Dehghani, Solid phase extraction of Cd (II) and Pb (II) using a magnetic metal-organic framework, and their determination by FAAS, Micro. Chim. Acta, 180 (2013) 589-597.

[15] J. Liu, T. Zhang, Z. Wang, G. Dawson, W. Chen, Simple pyrolysis of urea into graphitic carbon nitride with recyclable adsorption and photocatalytic activity, J. Mater. Chem, 21 (2011) 14398-14401.

[16] G. Li, N. Yang, W. Wang, W. Zhang, Synthesis, photophysical and photocatalytic properties of N-doped sodium niobate sensitized by carbon nitride, J. Phys. Chem. C, 113 (2009) 14829-14833.

[17] Y. Jia, D.-H. Kim, T. Lee, S. Kang, B. Lee, S. Rhee, C. Liu, One-pot solvothermal synthesis of magnetic SnFe 2 O 4 nanoparticles and their performance in the photocatalytic degradation of chlortetracycline

with visible light radiation, RSC. Adv, 6 (2016) 76542-76550.

[18] A. Moghimi, M. Alijanianzadeh, R. Pourahmad, Extraction and separation of Ni (II) from by functionalized graphene oxide with covalently linked porphyrin (GOH$_2$NP) adsorbed on surfactant coated C18, Afr. J. Pure Appl. Chem, 7 (2013) 360-369.

[19] M. Saraji, H. Yousefi, Selective solid-phase extraction of Ni (II) by an ion-imprinted polymer from water samples, J. hazard. mater, 167 (2009) 1152-1157.

[20] M.A. Karimi, M. Kafi, Removal, preconcentration and determination of Ni (II) from different environmental samples using modified magnetite nanoparticles prior to flame atomic absorption spectrometry, Arab. J. Chem, 8 (2015) 812-820.

[21] A. Ersöz, R. Say, A. Denizli, Ni (II) ion-imprinted solid-phase extraction and preconcentration in aqueous solutions by packed-bed columns, Anal. Chim. Acta, 502 (2004) 91-97.